

IBM Research Report

The time development of microstructure and resistivity for very thin Cu films

Stephen M. Rossnagel

IBM Research Division

Thomas J. Watson Research Center

P.O. Box 218

Yorktown Heights, NY 10598

Tung Sheng Kuan

Dept. Of Physics

University at Albany (SUNY)

Albany, NY 12222



Research Division

Almaden - Austin - Beijing - Delhi - Haifa - India - T. J. Watson - Tokyo - Zurich

The time development of microstructure and resistivity for very thin Cu films

S.M. Rossnagel and T.S. Kuan*

IBM Research Div, PO 218, Yorktown Heights, NY 10598

* Dept. Of Physics, University at Albany (SUNY), Albany, NY 12222

ABSTRACT

The electrical resistance of thin, 4-100 nm sputter-deposited (PVD) Cu films was measured in-situ in the deposition chamber. The Cu was deposited on silicon dioxide surfaces to reduce surface pinning or adhesion effects and allow high mobility. During, and following the deposition, the electrical resistance was measured under vacuum for periods of up to several thousand minutes, and in each case the electrical resistivity decreased 13-50% over that time period. This is consistent with reports of room temperature grain growth in electrodeposited thin films. XRD data showed significant increases in (111) crystallinity. At very small thicknesses (4.5 nm), it appears that a second mechanism occurs prior to grain growth which may be related to the agglomeration of nearly discontinuous islands on the surface. Similar Cu films deposited on Ta adhesion layers showed little, if any, change in resistance over time, indicating the role of the substrate interface in limiting grain growth.

INTRODUCTION

Changes in deposited Cu films at room temperature have been observed for over 30 years.

Initially, the observations were with thick, sputter deposited films which showed recrystallization and grain growth effects in nine to several hundred hours at room temperature (1). More recently, significant changes in film resistivity for electrodeposited Cu films have been reported (2-8), with resistivity dropping from 10-30% above the bulk value down to near-bulk in a few to tens of

hours, after a transient period of several hours. Much of that work was summarized by Harper et al (9), which attributed the resistivity decrease to abnormal grain growth driven by the relaxation of energy stored in the initially very small grain size, as-deposited films. The apparent activation energy for this process, estimated by Cabral et al (2) at about 0.9 eV and later by Jiang and Thomas (8) at approximately 0.8 eV, corresponds roughly with the activation energy for surface self-diffusion or for grain boundary diffusion in Cu (10).

In general, most of this latter work was with films of 1-3 micron thickness electrodeposited on PVD Cu seed layers of typically 100 nm or so in thickness. The initial grain size of the electrodeposited Cu was 50-100 nm. Using the Mayadas-Shatzkes (11) model for the effect of grain boundary scattering on film resistivity and the known 39 nm mean free path for electrons in Cu at room temperature, Harper et al predicted that a grain boundary scattering coefficient in the range of 0.2 to 0.4 would be sufficient to account for the observed resistivity decrease as the grain size grew from 50-100 nm up to several microns in a period of many hours (9). This value is similar to the 0.3 reported elsewhere (12).

In the work with electroplated films, each of the deposits was a several-micron-thick film deposited on top of a thin, sputter-deposited Cu seed layer. The seed layer typically has a fine-grained microstructure, and this appears to constrain the initial grain size of the electrodeposited material. One general characteristic of this structure is that the recrystallization effects do not occur immediately after electrodeposition, but may take many hours to begin. This is consistent with a process known as Ostwald ripening, in which the pinning species migrate along grain boundaries, followed by the unpinning of some boundaries which then allows

abnormal grain growth (9). Another characteristic is that the recrystallization effect occurs most readily with thick films, and much less rapidly, if at all, with very thin films, and the model of Harper suggest a transient time that is inversely proportional to film thickness (9).

The recrystallization effect was found to be minimal in films below 100 nm thickness or else lines less than approximately 250 nm in width, due probably to the dominance of the moderately-stable fine-grained PVD seed layer compared to the electrodeposited thickness. However, the current dimensions of damascene Cu lines in microelectronic applications are in the 130 to 180 nm range, and lines below 100 nm will be used in the near future. Since the as-deposited electrical resistance is 20-30% higher than bulk, it is of interest to determine whether thin, sub-100 nm Cu films can be recrystallized to attain closer to bulk resistivity and whether there are any practical means to accomplish this on a manufacturing scale. Currently, this problem is solved by pre-CMP annealing.

The current experiment examines Cu films, deposited only by sputtering, in the thickness range of 4 to 100 nm. A key difference between these measurements and those related to PVD seedlayers and electroplated films is that much of this work does not use an adhesion layer, such as Ta, under the Cu film. By depositing the Cu directly on a surface, such as silicon dioxide, to which the Cu has little, if any, adhesion, the recrystallization effects can occur without being pinned by the film-substrate interface. For comparison purposes, films were also deposited on Ta surfaces, to which the Cu should adhere, as well as air-exposed Ta surfaces, which is more similar to the silicon dioxide surface.

EXPERIMENT

The Cu films were sputter deposited in a mostly conventional, commercial PVD magnetron deposition chamber (Applied Materials Endura). This system has a 300 mm diameter magnetron cathode with a moving magnet assembly behind the cathode. The Cu cathode used was of the highest purity available (99.99999%). The system base pressure was 10^{-8} Torr, pumped by a cryopump, and the Ar used was UHP grade (99.9999%) at a working pressure of 0.5 mTorr with the main gate valve to the cryopump completely open. A grounded, physical collimator was used which extended across the entire midsection of the chamber between the cathode and the sample. Samples were introduced under the collimator via a loadlock.

The samples used were pieces of thermally oxidized Si wafers (500 nm oxide thickness) which were clamped to a specialized holder on the wafer-loading arm. (This part of the tool is markedly different than the commercial version.) On the samples, two parallel 250 nm thick Cu bands approximately 2 cm wide along with an underlying Ta adhesion layer were sputter-deposited with a spacing of 1 cm. The edges of the Cu bands were tapered such that further film deposition would be continuous over the edge of the band. Broad electrical leads were then attached to the bands prior to subsequent Cu deposition and the resistance of the wires and the contacts was measured. A thermocouple was located under the sample.

The deposition chamber was outfitted with a 1.5:1 aspect ratio hexagonal, grounded collimator.

This reduced the deposition rate compared to an open system at the sample by 5x, but more

importantly, eliminated any measurable flux of ions or electrons to the sample position, which was 5 cm below the collimator. Cu deposition was accomplished with a discharge power of 1000W and a rate of 8 nm/min at the sample location (under the collimator). A quartz crystal rate monitor was configured immediately adjacent to the sample on the centerline of the chamber and calibrated by comparison to step profiles measured on thicker films of 200 to 500 nm.

A dc voltage of 0.1 to 5 V was applied across the two Cu bands on the SiO₂ surface, and the current measured on a precision constant voltage power supply. The voltage was applied only for 0.2 to 0.5 seconds. This reduced concerns of ohmically heating the films, an effect which could be measured after several seconds, as well as any (unlikely) electromigration-like effects which might alter the film conductivity. The resistance of the wires from the power supply to the sample was measured, and wide-area clamped contacts to the film were used, such that the observed current and voltage could be converted into film resistivity. During deposition of the thin Cu films, the film thickness and electrical resistance were measured at 5 second intervals, and the applied voltage was switched off for the remainder of the period. Following deposition to some desired, terminal thickness, the resistance was measured at 5 second intervals for several minutes, and then with increasingly-longer time intervals over a period of up to several thousand minutes (days). The voltage was always off except for the actual measurement. These post-deposition measurements were made either in the deposition chamber or the load-lock, in either case under vacuum of 10⁻⁶ Torr or better. There was initial concern over general heating effects in the deposition chamber, but measurements with the thermocouple showed sample temperature changes of less than 1 degree C with a time constant for cooling after deposition of 1 second or less.

Cu films were sputter deposited on identical, but separate substrates to film thicknesses of 4.5, 9, 13.5, 18, 30 and 100 nm. Cu films were also deposited on silicon nitride coated Si wafer substrates as well as thin, silicon nitride TEM window structures. The thickness in each case was measured by the adjacent quartz crystal rate monitor, rather than by timing the deposition. As will become obvious below, the measured thickness was simply the average thickness inferred by the weight of the deposit and does not imply a uniform, continuous film over the substrate. For the substrate, silicon dioxide was chosen primarily because there is poor adhesion, if any, between Cu and SiO₂ and the Cu atoms are anticipated to be fairly mobile at the deposition temperature of 25°C. X-ray diffraction (XRD) results were obtained post-deposition using a Phillips theta-two-theta system.

RESULTS

The primary observables in this experiment are (a) the average deposition thickness measured by the quartz crystal microbalance adjacent to the sample, and (b) the current passed through the film at the constant applied voltage. Due to the finite resistance in the leads and contacts, the real voltage across the Cu bands on the sample is a function of the current. However, this is only critical in determining the absolute resistivity, and less important to observing changes in the films over time. For a film of 100 nm of Cu on SiO₂, the data are plotted in Figure 1 as a function of time. The rate monitor thickness data shows a linear increase with time until the deposition is stopped, and then no further changes with time. The current through the depositing films shows a lag up to about 4 nm where the film is apparently discontinuous and no current is passed. The

current then climbs rapidly as the thickness increases. However, when the deposition is stopped, the current continues to climb over the following several thousand minutes, increasing by 13% or so and eventually saturating.

The post-deposition change in the current through the film sample is somewhat dependent on the film thickness. Similar data of thickness and current as a function of time are shown in Figs 2 and 3 for terminal film thicknesses of 13.5 and 4.5 nm. For the 13.5 nm deposition, the current increased nearly 20% after 1000 minutes and was probably not at the final saturation value when the measurement was terminated (Fig. 3). For the case of the 4.5 nm Cu film, which is barely continuous, the current through the film increased by nearly 100% over 1000 minutes and was also probably not at completion when the experiment was ended (Fig. 3).

The dc resistance of the Cu films could be calculated from the voltage applied to the leads and the current through the film, modified by the resistance of the leads and contacts to the film. For these connections, the resistance was measured from the Cu electrode pads on the sample for each sample to account for differences in contact resistance. Nevertheless, the accuracy of this type of measurement is modest and the uncertainty in the observed resistivities is estimated at nearly 20%. The resistivities were calculated as a function of time for each of the films measured (4.5, 9, 13.5, 18, 30 and 100 nm) and the thinner films are plotted in Fig. 4. The data show an initial systematic reduction in film resistivity as a function of film thickness, due mostly to electron-surface scattering (13). In each case, the resistivity with time then decreased with approximately the same slope with time. The exception was the 4.5 nm film, which was barely

continuous, and showed a more-steep drop in resistivity for the first 10 minutes following deposition.

Ex-situ XRD observations of similar samples made under the same conditions as the in-situ resistance measurements showed significant changes in the crystallinity of the films over time. The films at all thicknesses were predominantly (111) oriented with a small (200) component. Over extended periods of time consistent with the change in resistivity observed, the (111) peak increased almost an order of magnitude and the FWHM reduced by 50%, (Fig. 5) consistent with grain growth but no change in orientation. The degree of increase in the crystallinity was also related to whether the sample was held in room air or in vacuum. Samples stored in vacuum tended to have a slightly narrower (111) peak (Fig. 5b), and in some cases, the (111) peak height was greater than similar samples stored in air. Cu films deposited on silicon nitride surfaces showed essentially the same results as depositions on silicon oxide.

To determine the effect of an adherent substrate, Cu films were deposited onto 3 nm Ta underlayers, both in-situ and also with an air exposure between the Ta and Cu depositions. For the in-situ case, a Cu film of 18 nm was deposited immediately following the Ta deposition although it was not possible to measure the current through the film during the Cu deposition.. Following the deposition, the resistivity was measured over a period of up to 1000 hours in a nitrogen ambient. Within the accuracy and reproducibility of the 4-pt probe technique, there was less than a 3% reduction in the Cu resistivity over that period. A similar experiment was done for a Ta film which was exposed to air prior to the deposition of the 18 nm Cu film. In this case,

the resistivity of the Cu film decreased at room temperature in a nearly identical way to the Cu films deposited on silicon dioxide samples.

Thin, 30 nm Cu films for TEM analysis were deposited on 50 nm silicon nitride membranes mounted on small etched-Si window structures. Immediately following deposition, the samples were inserted in the TEM and the microstructure observed at low beam current for a brief period of time. The initial microstructure was random, polycrystalline grains with a maximum lateral dimension of 25 nm. The sample was left in the TEM under vacuum with the electron beam off and the sample was observed at 20 minute time intervals for up to 46 hours following deposition (Fig. 7). TEM observations indicated that grain rotation occurs actively within the first few hours and that grain growth is much less prominent and operating on a longer time scale. TEM image sequences suggest that a particular grain rotates first prior to size growth. The dark grains are non-(111) grains and most grain rotations observed are rotations toward (111) orientation. (A (111)-textured grain does not excite strong (002) and (111) reflections and thus appears bright in transmission). Both grain rotation and grain size growth contribute to the narrowing and intensity increase of (111) peak, but TEM results suggest that it is grain rotation that is responsible for the initial stage of resistivity decrease.

DISCUSSION

The results of the electrical measurements on the PVD Cu films deposited on SiO₂ surfaces show a significant reduction in the film resistivity as a function of time at room temperature for films

held both in air as well as in vacuum. This general trend is consistent with numerous earlier reports, both with PVD and electroplated Cu films, which also showed 10-30% reductions in resistivity in the hours following deposition.

The effect appears to scale roughly inversely with film thickness; a result which is the opposite of that reported earlier with electroplated films. The magnitude of the resistance change 1000 minutes post-deposition, compared with the as-deposited value is shown in Fig. 6.

XRD observations of these and companion films show a strong (111) preferred orientation to the films. Over time, consistent with the observed changes in electrical resistivity, the (111) peak increases significantly in intensity (roughly 10x for an 18 nm Cu film), and its FWHM reduces by 50%; both consistent with extensive grain growth in the films. These effects were observed for films held in air as well as under vacuum. There was a slightly larger reduction in the (111) FWHM for films stored under vacuum, but fairly little change in the (111) intensity, suggesting that film oxidation is not a rapid process for these very thin films. This was also somewhat unexpected, and 10-18 nm films showed no evidence of oxidation, in terms of either increased resistivity or degraded (111) orientation after 5 days in room air at 25C.

When an adhesion layer, Ta, was used under the Cu film, the recrystallization effects were markedly reduced. There was less than a 3% reduction in the resistivity for a 18 nm film over a period of >1000 hrs and no observable change in the XRD peak heights or widths. When the Cu films were deposited on a Ta layer which had been air-exposed, the changes in resistivity and crystallinity were identical to Cu samples on a bare SiO₂ surface. This suggests that

contamination of the Cu-Ta interface will most likely (1) reduce Cu adhesion, (2) allow recrystallization of the Cu, and (3) allow other surface-diffusion-like effects to occur at the Cu-Ta interface. This last item will probably facilitate electromigration effects in Cu interconnect structures.

CONCLUSIONS

Room temperature recrystallization of very thin PVD Cu films has been observed on Cu films which are poorly adherent to the substrate. The recrystallization effect occurs over a period of hours to hundreds of hours for films of 4.5 to 100 nm thickness, and is evident by a significant reduction in the film resistivity as well as strong increases in (111) peak height and reductions in peak width. The effect scales roughly inversely with film thickness, indicative of a surface-diffusion-driven process.

REFERENCES

1. J. W. Patten, E.D. McLanahan and J.W. Johnston, *J. Appl. Phys.*, **42** (1971) 4371.
2. C. Cabral, Jr., et al, *Proc. Adv. Metall. Conf*, **14** (1999) 81.
3. T. Ritzdorf, L. Graham, S. Jin., C. Mu and D.B. Fraser, *Proc. of the International Interconnect Technology Conference (IITC) (IEEE, New York, 1998)* p. 166.
4. M. E. Gross et al., *Mater. Res. Soc. Symp. Proc.* **514** (1998) 293, M. E. Gross, K. Takahashi, T. Ritzdorf, and K. Gibbons, *Proc. Adv. Metall. Conf.*, Colorado Springs (1998).
5. V. M. Dubin, G. Morales, C. Ryu and S. S. Wong, *Mater. Res. Soc. Symp. Proc.* **505** (1998) 137.
6. Q. -T. Jiang, R. Mikkola, B. Carpenter and M. E. Thomas, *Proc. Adv. Metall. Conf*, Colorado Springs (1998).
7. L. M. Gignac, K. P. Rodbell, C. Cabral. Jr., P. Andricacos, P. M. Rice, R. B. Beyers, P. Locke and S. J. Klepsis, *Mater. Res. Soc. Symp. Proc.*, **562** (1999) 209.
8. Q.-T. Jiang and M. E. Thomas, *J. Vac. Sci. & Technol*, **B19** (2001) 762.
9. J. M. E. Harper, C. Cabral Jr., P.C. Andricacos, L. Gignac, I. C. Noyan, K. P. Rodbell and C. K. Hu, *J. Appl. Phys.* **86** (1999) 2516.

10. D. Gupta, Mater. Res. Soc. Symp. Proc., **337** (1994) 209.
11. A. F. Mayadas and M. Shatzkes, Phys. Rev. **B1** (1970) 1382.
12. T. S. Kuan, C. K. Inoki, G. S. Oehrlein, K. Rose, Y. -P. Zhao, G. -C. Wang, S. M. Rossnagel and C. Cabral Jr., Mater. Res. Soc. Symp. Proc., **612** (2000) D7.1.1.
13. C. Kittel, Introduction to Solid State Physics, (John Wiley and Sons, 1953, New York), Chapter 7.

FIGURE CAPTIONS

Figure 1. Film thickness (left side) measured by quartz crystal microbalance and current through the film (right side) at constant applied voltage (to the leads) as a function of time. The deposition was terminated at 100 nm (1000 Å) thickness after a deposition time of 20 minutes.

Figure 2. Film thickness (squares) and current through the film (diamonds) as a function of time for a deposition terminated at 13.5 nm (135 Å). The horizontal line shows the current at the termination of the deposition (390 mA).

Figure 3. Film thickness (squares) and current through the film (diamonds) as a function of time for a deposition stopped at 4.5 nm (45 Å). The dotted line shows the current at the termination of the deposition.

Figure 4. Measured Cu resistivity as a function of time for films of 4.5, 9, 13.5, 18 and 30 nm thickness.

Figure 5: (upper) XRD peak height for Cu (111) diffraction peak as a function of time following deposition for a 38 nm Cu film deposited on silicon dioxide at 25C. Data points are for two samples stored in air, measured sequentially (shown as points connected by lines), and for individual samples stored up to the time of measurement in vacuum (shown as individual, open circles). (lower) (111) FWHM as a function of time for the same cases as the upper plot.

Figure 6. The ratio of the film resistance (and resistivity) 1000 minutes following the deposition compared with the resistance as-deposited, plotted as a function of the average film thickness. The Cu films were deposited on SiO₂ surfaces at 25C and held at 25 C under vacuum in the deposition chamber.

Figure 7. (a) Bright-field TEM image of 30 nm Cu film taken 0.6 hr after deposition on a silicon nitride membrane. (b) Image of the same area as in (a) taken 2.3 hr after film deposition. “R”

marks the rotated grains. (c) Image of the same area as (a) and (b) taken 46.5 hr after film deposition. "G" marks the grown grains.

Figure 1

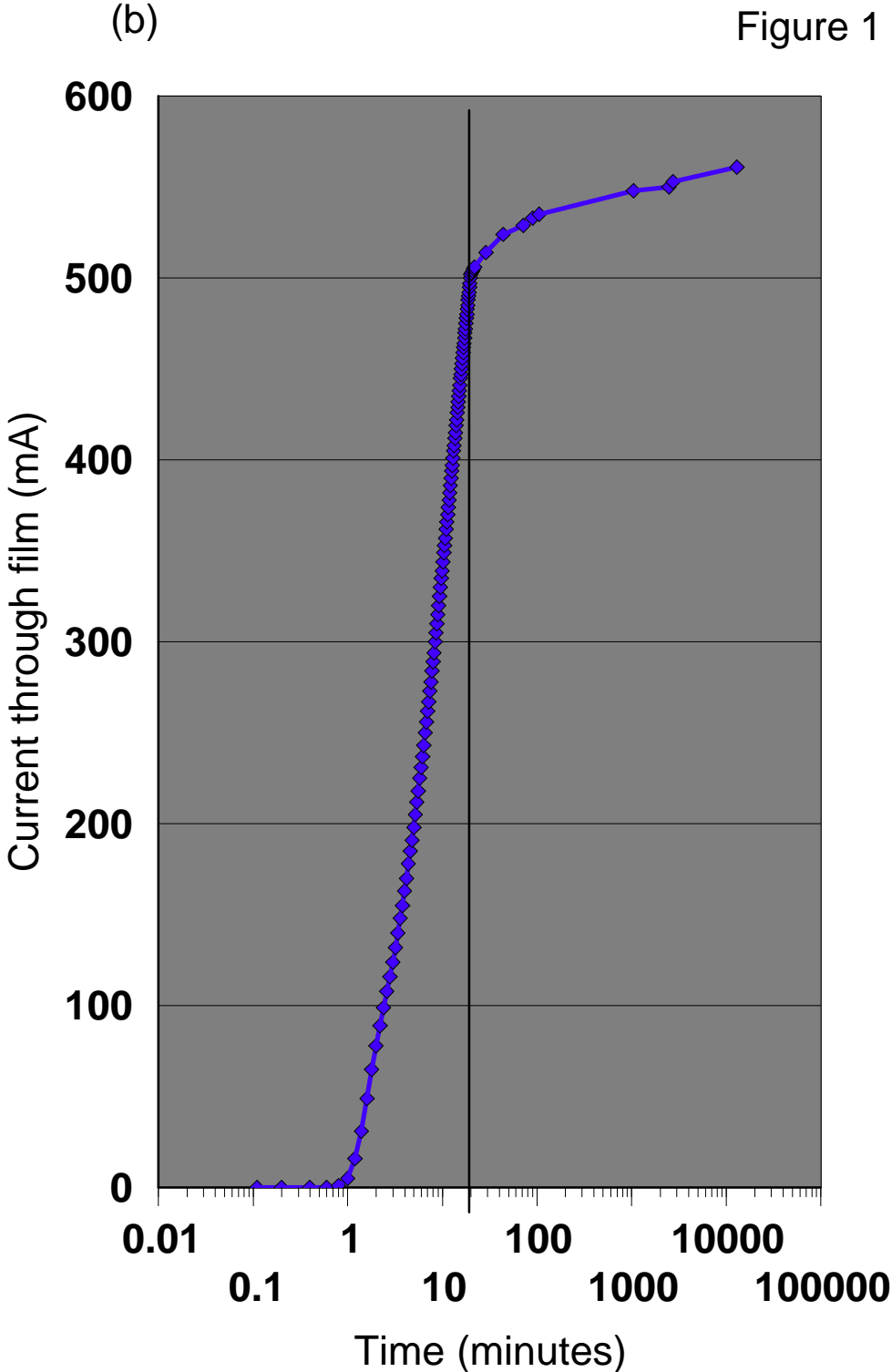
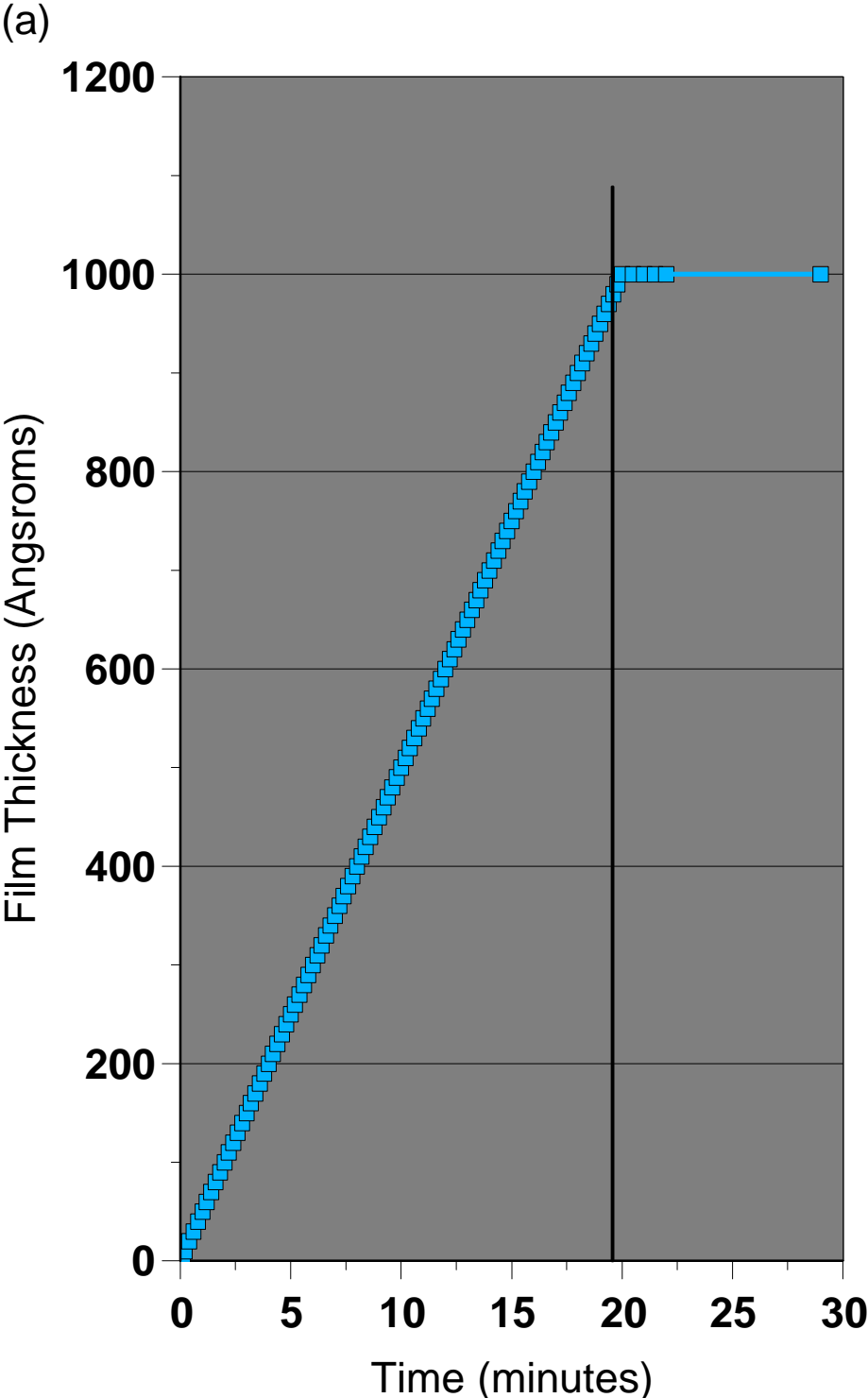


Figure 2

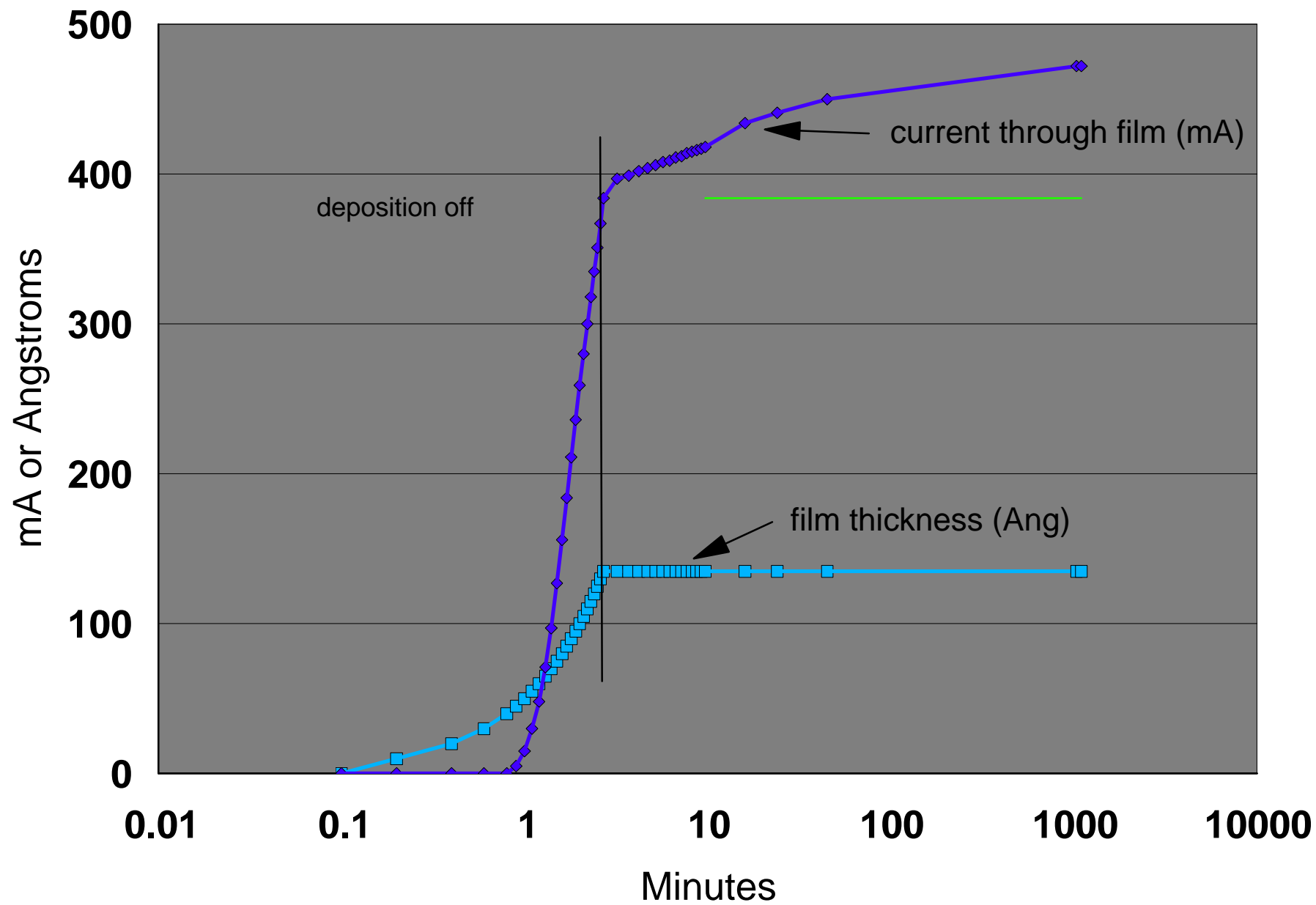


Figure 3

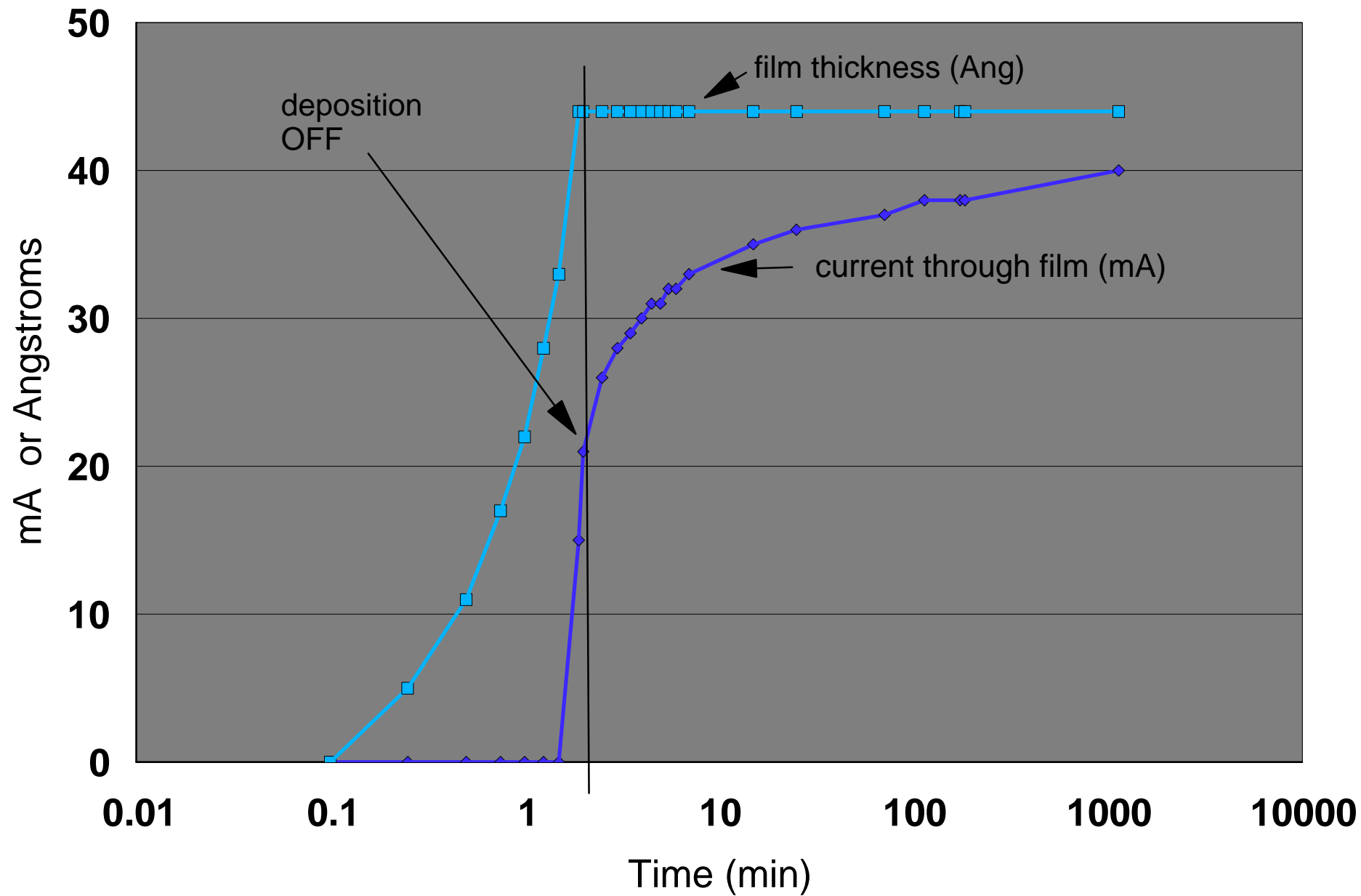


Figure 4

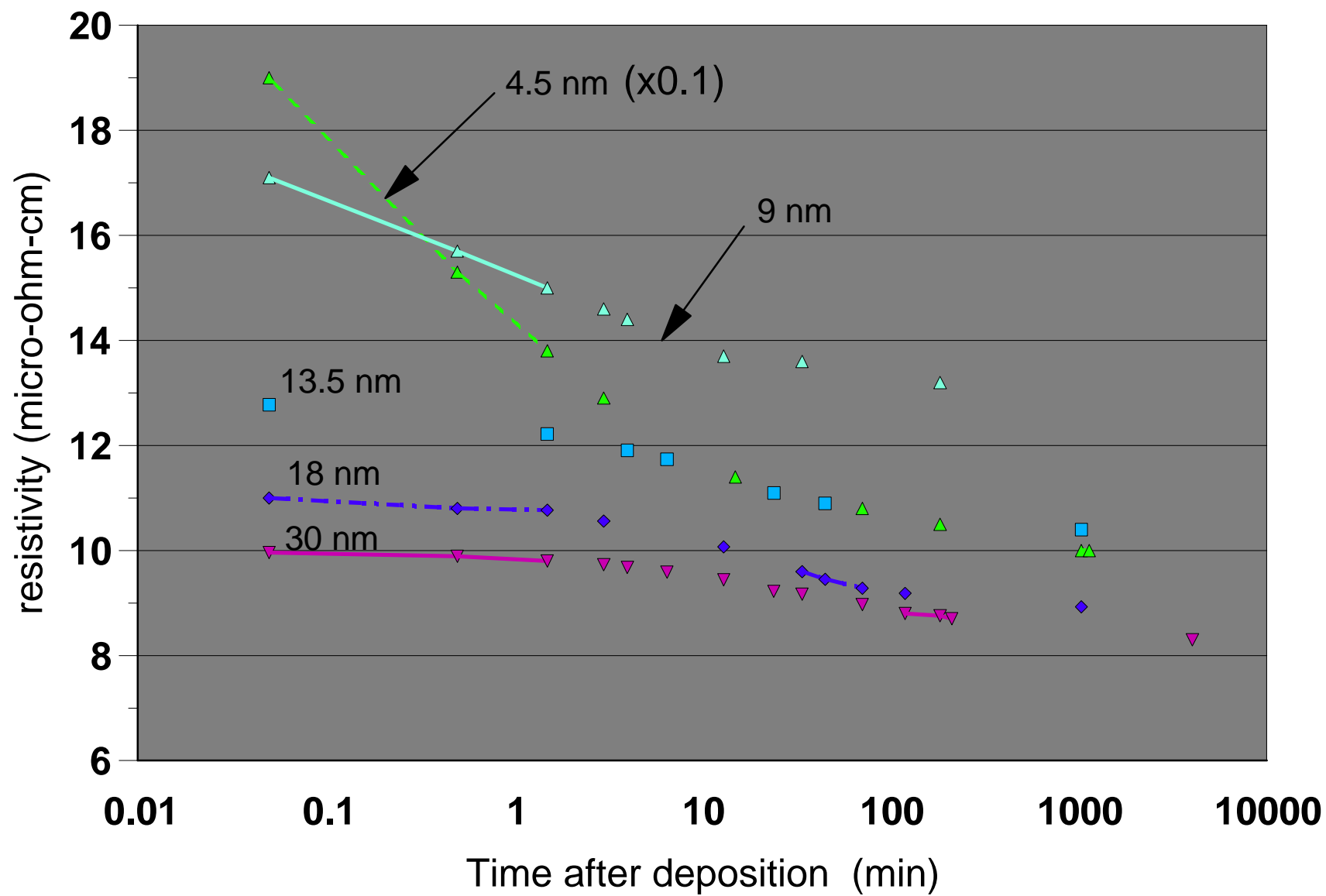


Figure 5(a)

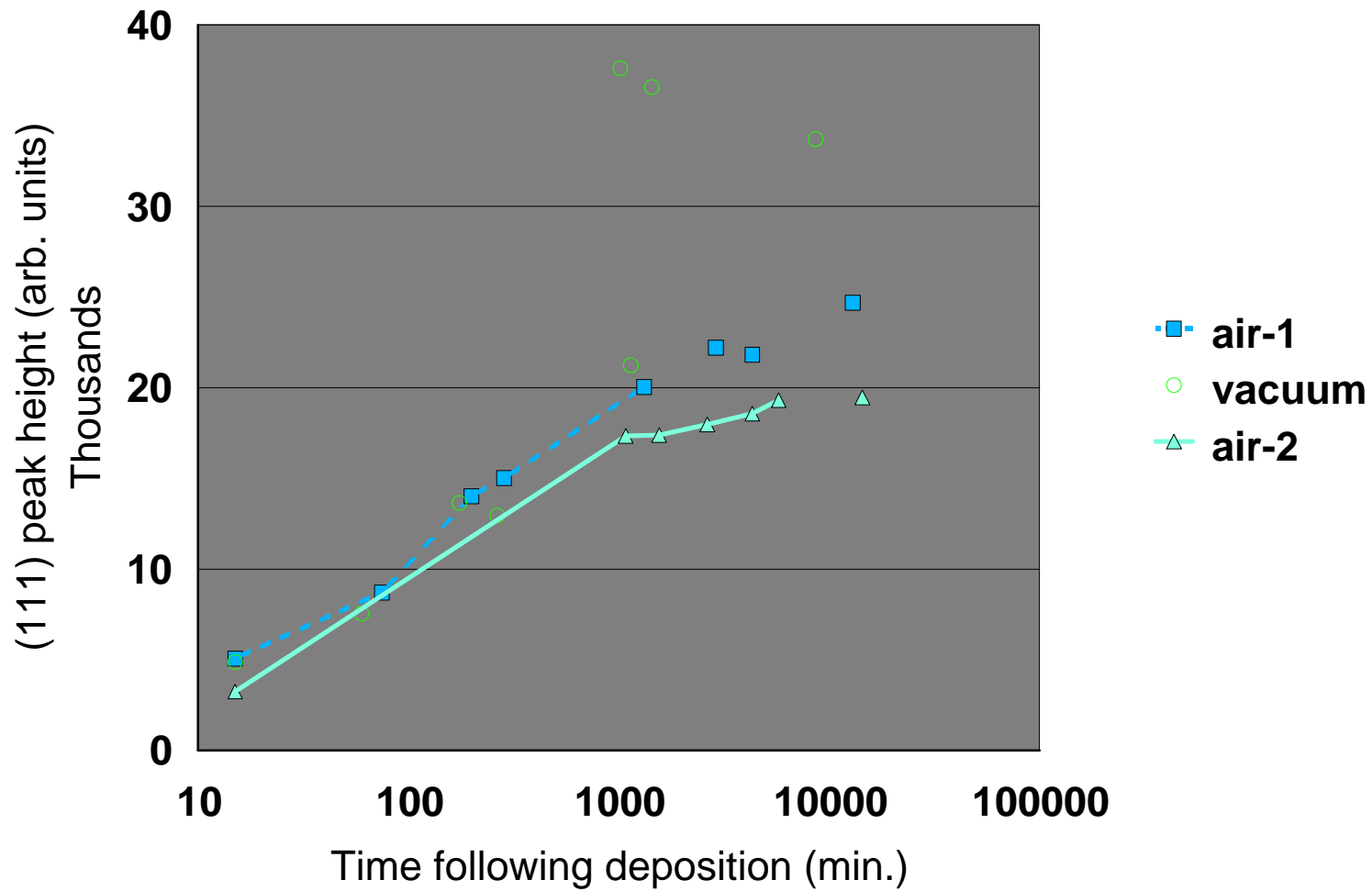


Figure 5(b)

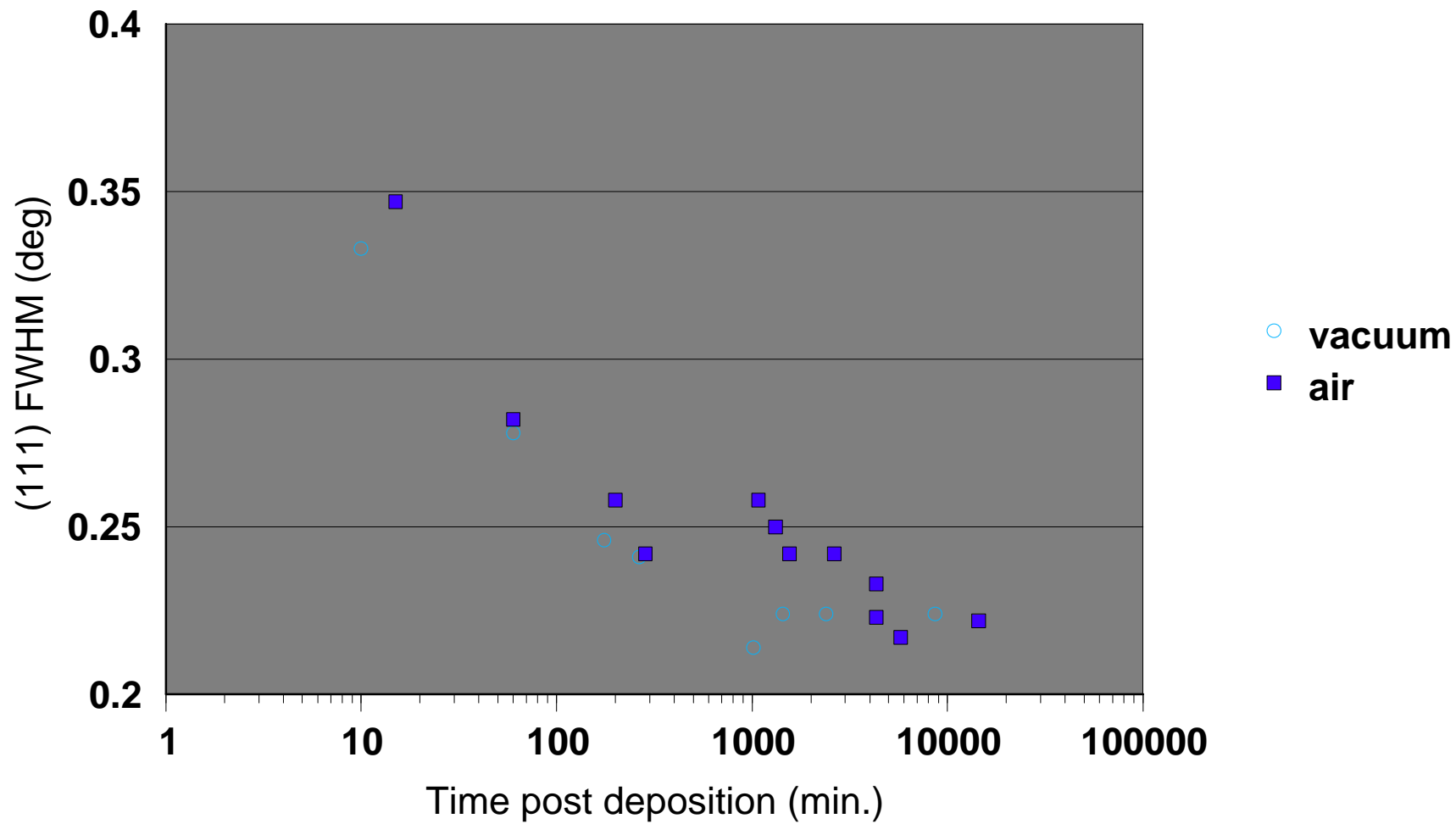


Figure 6

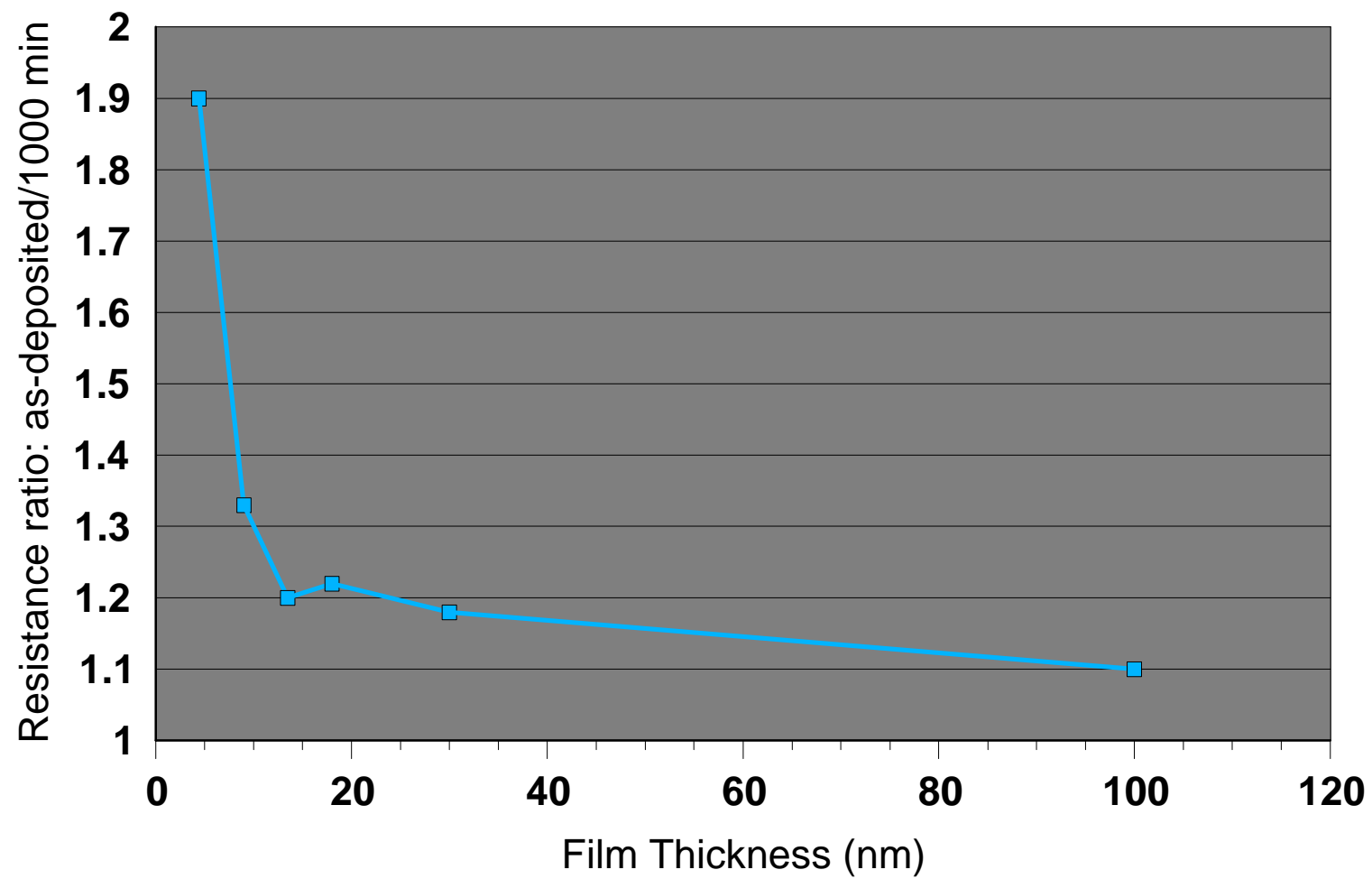
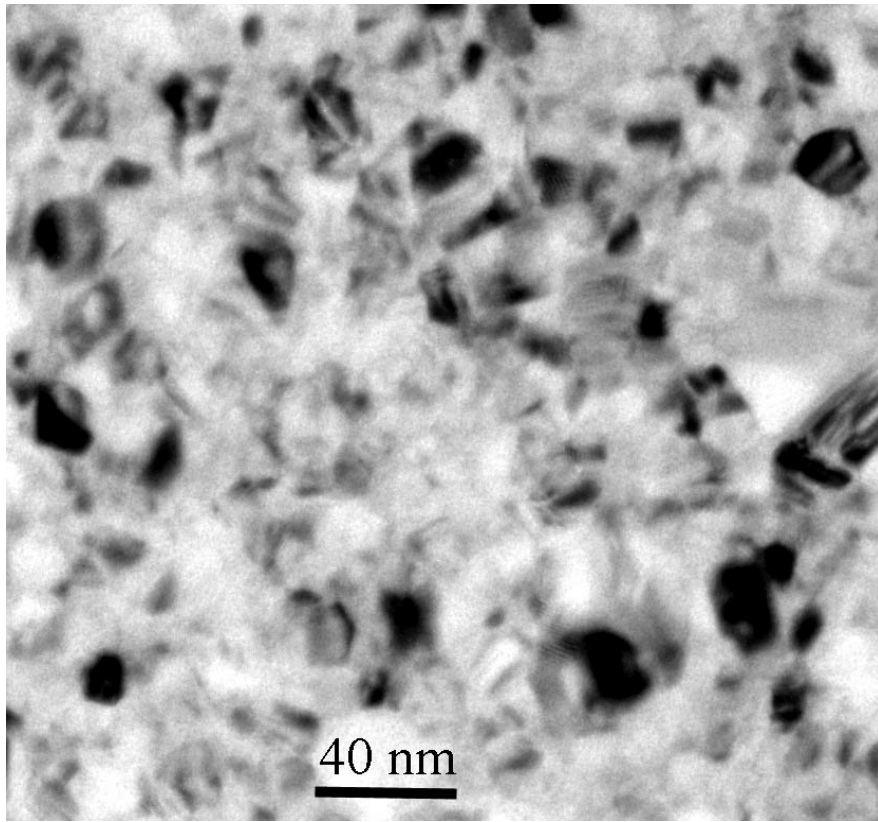


Fig. 7 (a)



(b)

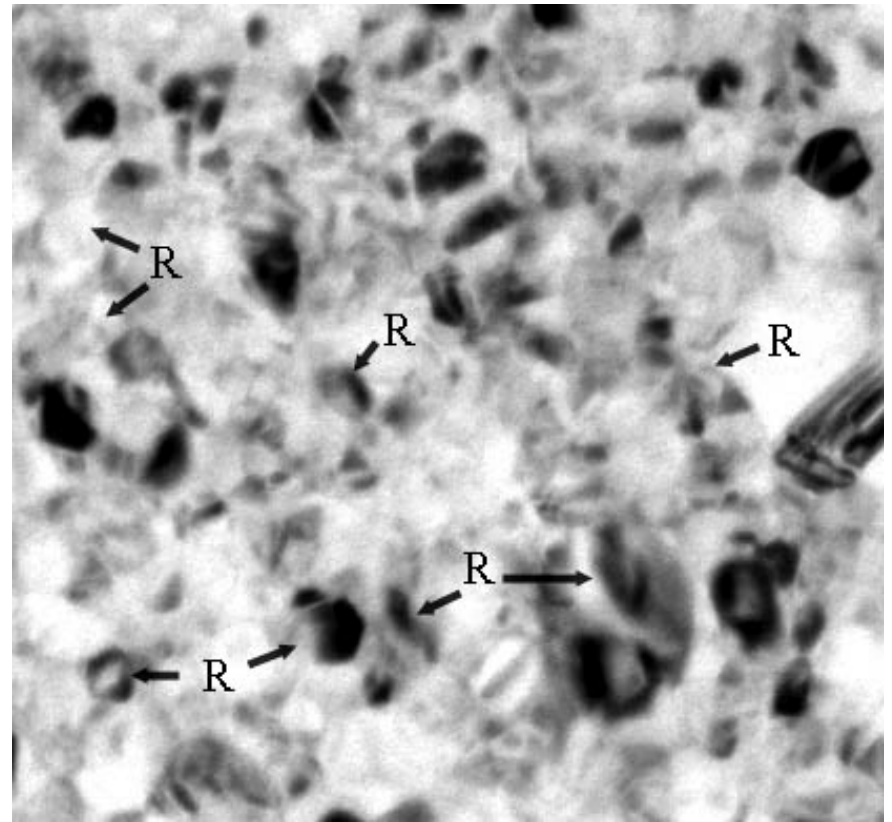


Fig. 7 (c)

